

Optimal Fine-Grained N:M sparsity for Activations and Neural Gradients

Brian Chmiel ^{*1,2} Itay Hubara ^{*1,2} Ron Banner ¹ Daniel Soudry ²

Abstract

In deep learning, fine-grained N:M sparsity reduces the data footprint and bandwidth of a General Matrix multiply (GEMM) by x2, and doubles throughput by skipping computation of zero values. So far, it was only used to prune weights. We examine how this method can be used also for activations and their gradients (i.e., "neural gradients"). To this end, we first establish tensor-level optimality criteria. Previous works aimed to minimize the mean-square-error (MSE) of each pruned block. We show that while minimization of the MSE works fine for pruning the activations, it catastrophically fails for the neural gradients. Instead, we show that optimal pruning of the neural gradients requires an unbiased minimum-variance pruning mask. We design such specialized masks, and find that in most cases, 1:2 sparsity is sufficient for training, and 2:4 sparsity is usually enough when this is not the case. Further, we suggest combining several such methods together in order to speed up training even more. A reference implementation is supplied in <https://github.com/brianchmiel/Act-and-Grad-structured-sparsity>.

1. Introduction

Over the past decade, deep neural networks (DNNs) achieved profound success in many fields including, computer vision and natural language processing. However, training such state-of-the-art DNNs may necessitate thousands of petaflops and many Gigabytes of storage to contain trillions of parameters. Thus, researchers from academia and the industry are actively seeking new techniques to reduce the power and increase the throughput of DNNs models for both training and inference. The main techniques in

^{*}Equal contribution ¹Habana Labs – An Intel company, Caesarea, Israel ²Department of Electrical Engineering - Technion, Haifa, Israel. Correspondence to: Brian Chmiel <bchmiel@habana.ai>.

this area include quantization, knowledge distillation, and pruning.

Pruning DNNs is one of the most effective and widely studied methods to improve DNN resource efficiency. Since DNNs are over-parametrized most researchers focused on weights pruning. Yet, recently researchers suggested that sparsity of activation (Jaszczur et al., 2021; Kurtz et al., 2020) and gradients (Chmiel et al., 2021b) could be exploited as well. All these types of *unstructured* pruning only reduce the memory footprint (Frankle & Carbin, 2018; Evcı et al., 2020). It is possible to also reduce the compute footprint by enforcing some structure such as block sparsity (Wen et al., 2016), filter sparsity (Li et al., 2017), or N:M fine-grained sparsity (Nvidia, 2020; Hubara et al., 2021; Mishra et al., 2021).

N:M fine-grained sparsity can be used in one of Nvidia's sparse tensor cores (Nvidia, 2020; Mishra et al., 2021) in order to accelerate matrix multiplication. N:M fine-grained sparsity requires that, at least for one of the two matrices involved in the matrix multiplication, N out of every M contiguous elements would be pruned. For example, Nvidia demonstrated (Nvidia, 2020) a 2:4 format can accelerate inference by x2. They suggested using a three-step scheme: (a) train a dense model, (b) prune weights to obtain a fine-grained 2:4 fixed mask, and (c) use the original training regime to retrain with the masked weights.

Following work suggested methods to accelerate different parts of this scheme. First, Zhou et al. (2021) was able to omit steps (a) and (b) by training with an N:M mask from scratch using a straight-through estimator (STE) and additional regularization. Specifically, they keep a dense copy of the weights and set different weight decays rates to the masked and unmasked weights

Next, Hubara et al. (2021) focused on accelerating the remaining step (c), i.e., sparse training. Generally, there are three General Matrix Multiplications (GEMMs) involved in a training step of a single DNN layer: (1) forward pass with a GEMM between the weights and activations, (2) backward pass with a GEMM between the gradients and transposed weights, and (3) update phase with a GEMM between the gradients and activations. While Nvidia suggested accelerating only the inference phase (i.e., the forward pass), the backward and update passes were kept dense. Noting

that the backward phase uses the transposed (sparse) weight matrix, [Hubara et al. \(2021\)](#) used a transposable mask, i.e., a mask that can be transposed and still match the N:M fine-grained structure. This enabled the acceleration of the backward phase. Although [Hubara et al. \(2021\)](#) suggested different methods to find the optimal transposable mask efficiently, they did not offer ideas on how to accelerate the update phase matrix multiplication.

In this work we explore different methods to accelerate the update phase as well. To that end, we examine gradients with fine-grained pruning and establish a tensor-level optimality criteria. Our experiments suggest that while the traditional method crashed, our method with 1:2 sparsity is sufficient for training, and 2:4 sparsity is usually enough when this is not the case. Moreover, we suggest to combine several such methods together (fine-grained sparse gradient and sparse transposable fine-grained weights) in order to speed up training even more and for the first time accelerate all training phases with N:M fine-grained sparsity. Moreover, we studied the effect of applying N:M structured sparsity on the activations and showed results of N:M fine grained sparsity for inference that are equivalent to 2-bit quantization achieving on par results. In Table 1 we summarize all the N:M fine-grained structured sparsity methods, which part of the network they accelerate and the relevant optimality criteria we use. Additionally, we showed the configurations used to fully accelerate training or inference.

This paper makes the following contributions:

- We developed unbiased minimum variance optimality criteria for pruning neural gradients with N:M structured sparsity.
- We propose 1:2 and 2:4 unbiased minimum variance methods to prune the neural gradients and demonstrate that they achieve small or no degradation where previous methods failed.
- We are able to speed up training by 2x for the first time with our new method combined with previous methods of N:M structured sparsity.
- We show combining N:M sparsity for activations and weights, together with 4-bit quantization achieves on par results with quantization-aware-training results for 2-bit inference.

2. Related works

Pruning has been extensively investigated in the last few years. Most of the pruning methods focus on pruning of the weights ([Evci et al., 2020](#); [Frankle & Carbin, 2018](#); [Janowsky, 1989](#); [Liu et al., 2018](#)). Unstructured pruning

Table 1. Exploring fine-grained sparsity on different tensors (activations,weights,gradients) and with different sampling methods (MVUE, MSE). For inference scheme we used sparse weights and activations and for our training scheme we used transposable weights and sparse gradients.

Phase Tensor \	Forward	Backward	Update
Weights (Nvidia, 2020)	✓(MSE)	✗	✗
T-Weights (Hubara et al., 2021)	✓(MSE)	✓(MSE)	✗
Activations (ours)	✓(MSE)	✗	✗
Gradients (ours)	✗	✗	✓(MVUE)
Inference Config. Weights+Activations	✓(MSE)	✗	✗
Training Config. T-Weights+Gradients	✓(MSE)	✓(MSE)	✓(MVUE)

methods achieved impressive sparsity ratio with minimal or no accuracy degradation, e.g. [Renda et al. \(2020\)](#) achieved over 80% sparsity in ResNet50- ImageNet dataset without sacrificing accuracy. Despite this impressive achievement, the ability of unstructured pruning methods to actually reduce computational resources of modern hardware is limited ([Nvidia, 2020](#); [Mishra et al., 2021](#)).

Structured pruning methods vary between coarse-grained and fine-grained methods. Coarse-grained methods such as filter-wise or layer-wise pruning ([Li et al., 2017](#); [Luo et al., 2017](#); [Wen et al., 2016](#)) are naturally supported by hardware and software but none of these methods were able to maintain the test accuracy for sparsity ratio higher than 50%. Recently, Nvidia introduced the Ampere GPU architecture ([Nvidia, 2020](#); [Mishra et al., 2021](#)) hardware with software support for N:M fine-grained structured sparsity. Specifically, they showed that 2:4 fine-grained structured sparsity, where two of every four contiguous elements are zero, achieves a 2x improvement in the GEMM operation. They suggested a three-step scheme to accelerate inference. Later, [Zhou et al. \(2021\)](#) accelerated their method by avoiding the first two steps. Next, [Hubara et al. \(2021\)](#) accelerated the remaining training step by suggesting transposable mask, which accelerates both the forward and backward phases ($\frac{2}{3}$ of the training). [Stosic & Stosic \(2021\)](#) further demonstrated the transposable mask can accelerate training with minimal accuracy degradation on 20 different models for various tasks and datasets. [Pool & Yu \(2021\)](#) suggested permuting the weight matrices to improve accuracy of sparse models for inference. [Sun et al. \(2021\)](#) suggested a mixed layer-wise N:M sparsity schemes to improve the uniform sparsity scheme with similar complexity constraints. [Holmes et al. \(2021\)](#) suggests a new learning framework to improve the performance of N:M sparse NLP models on downstream

tasks.

Beyond pruning the weights, recent work also focuses on unstructured sparsity of the activations or neural gradients. [Kurtz et al. \(2020\)](#) suggested a parametrized activations function called Forced-Activation-Threshold Rectified Linear Unit (FATReLU) which increases the naturally sparse of ReLU with any accuracy loss. [Jaszczur et al. \(2021\)](#) studied the sparsification of the activations in Transfomer-based models. "MeProp" ([Sun et al., 2017](#)) prunes the K smallest absolute-valued entries of the neural gradients on the fly, using the top-k algorithm. [Aamir Raihan & Aamodt \(2020\)](#) used top-k pruning on the copies of weights and activations used in the backpropagation. [Ye et al. \(2019\)](#), suggested "stochastic pruning", reaching higher sparsity levels on the neural gradient. [Chmiel et al. \(2021b\)](#) improved their results with a lognormal distribution approximation for the neural gradient achieving more than 80% sparsity on the neural gradients without accuracy degradation.

In parallel to our work, [McDanel et al. \(2022\)](#) suggested a method to use N:M structured data pruning for the neural gradients to accelerate the backward phase, which was also accelerated in [Hubara et al. \(2021\)](#). In Appendix A.4 we show the degradation of applying [McDanel et al. \(2022\)](#) method also in the update phase. As far as we know, no previous work suggested using N:M fine-grained sparsity to accelerate the update phase, by pruning the neural gradients. Moreover, we are the first work that suggest to use N:M fine grained sparsity on the activations to accelerate inference.

3. Which optimality criteria to use?

When pruning weights during training, we require local (tensor level) criteria to select which weights to prune. Recently, [Chmiel et al. \(2021a\)](#) investigated which optimality criteria to use, but in the context of quantization. They found, that when quantizing the activations, we should minimize the mean-square-error (MSE) of the quantization error. In contrast, for the neural gradients, they found that it is much more critical to use unbiased quantization (stochastic rounding). Based on their findings, we suggest to apply N:M fine-grained sparsity on the activations and neural gradients with the same optimality criteria:

(1) For the activations we focus on reducing the MSE. This is done with the greedy method of keeping the $M - N$ largest elements in each block of size M . Exploiting the inherent ReLU unstructured sparsity we experiment with forcing this form structured sparsity to vision models with ReLU activation functions, as discussed in section Section 6.3.

(2) For the neural gradients we focus on finding an unbiased estimator. From all the possible unbiased estimators, we will prefer the one that reduce the MSE. The MSE can be represented as follows: for a random variable x and a N:M

sparsity operator θ we can write $\text{MSE}[\theta(x)] = E[\theta(x) - x]^2 = \text{Var}[\theta(x)] + \text{Bias}^2[\theta(x)]$. Since we focus on an unbiased estimator (i.e., $\text{Bias}[\theta(x)] = 0$), we arrived to the optimality criteria of the minimum variance unbiased estimator (MVUE) for the neural gradients.

4. N:M Minimum variance unbiased estimator

In this section, we propose two unbiased estimators with minimum variance. The first corresponds to the 1:2 case and the second to the 2:4 case.

4.1. Minimum variance unbiased estimator for 1:2

For a block $[a, b]$, one entry needs to be pruned:

$$\theta([a, b]) = \begin{cases} [v_1, 0] & , \text{w.p. } p \\ [0, v_2] & , \text{w.p. } 1 - p \end{cases} \quad (1)$$

We wish to design an unbiased estimator for this pruning method where $E[\theta([a, b])] = [a, b]$:

$$E[\theta([a, b])] = p \cdot [v_1, 0] + (1 - p) \cdot [0, v_2] = [a, b] \quad (2)$$

To find an unbiased estimator which minimizes the total block variance, we now calculate the variance for each element in the block $\theta([a, b]) = [x, y]$ as follows:

$$\begin{aligned} \text{Var}[x] &= E[x^2] - E^2(x) = v_1^2 \cdot p - a^2 \\ \text{Var}[y] &= E[y^2] - E^2[y] = v_2^2 \cdot (1 - p) - b^2 \end{aligned} \quad (3)$$

Then, the total variance of a block is the sum of its element variances:

$$\text{Var}_B[\theta] = \text{Var}[x] + \text{Var}[y] = v_1^2 p - a^2 + v_2^2 (1 - p) - b^2 \quad (4)$$

Using equations 1 and 4 together we obtain the following expression for the total variance in the block specified by v_1 alone (for more information, see Appendix A.1):

$$\text{Var}_B[\theta] = v_1 \cdot a - a^2 + \frac{b^2 \cdot v_1}{v_1 - a} - b^2 \quad (5)$$

By finding the derivative of equation 5 with respect to v_1 and setting it to zero we get the following equation:

$$\frac{\partial \text{Var}_B[\theta]}{\partial v_1} = \frac{b^2}{v_1 - a} - \frac{b^2 v_1}{(v_1 - a)^2} + a = 0 \quad (6)$$

The solution to Equation 6 gives the following unbiased estimator, which has the lowest variance of all unbiased estimators (full details in Appendix A.1).

$$\theta([a, b]) = \begin{cases} [\text{sign}(a) \cdot (|a| + |b|), 0] & , \text{w.p. } \frac{|a|}{|a| + |b|} \\ [0, \text{sign}(b) \cdot (|a| + |b|)] & , \text{w.p. } \frac{|b|}{|a| + |b|} \end{cases} \quad (7)$$

Let us calculate the mean square error of this unbiased method. By substituting into Equation 5 the optimal solution for v_1 , the optimal method outlined in 7 has a variance of $2ab$. Therefore, since the method is unbiased it results with a mean-square-error of

$$\text{MSE} = \text{Bias}^2 + \text{Var} = 0 + 2ab = 2ab \quad (8)$$

In Table 2 we compare different 1:2 structured sparsity on the neural gradients on ResNet18 Cifar10 dataset. We show that although the proposed MVUE method doesn't minimize the MSE, it gets the best results.

Table 2. 1:2 sparsity on the neural gradients of ResNet18 cifar10 dataset. 'Greedy' refers to the traditional method of choosing the smallest element for each block. 'Biased' refers to the case $[v_1, v_2] = [a, b]$ in Equation (1). 'Uniform' refers to uniform sample, i.e. $p = 0.5$, $[v_1, v_2] = [a, b]$. 'Unbiased' refers to unbiased uniform sample, i.e $p = 0.5$, $[v_1, v_2] = [2a, 2b]$. 'MVUE' refers to the minimum variance unbiased estimator of Equation (7).

Method	Accuracy (%)
Baseline	90.02
Greedy	85.5
Biased	71.8
Uniform	85.8
Unbiased	87.2
MVUE (Ours)	89.98

4.2. Optimality criteria for 2:4

We now extend the results from the previous section to 2:4. With a block $[a_1, a_2, a_3, a_4]$, we wish to construct an unbiased 2:4 block with minimum variance. It can be seen that by assigning for each index i an element $\frac{a_i}{p_i}$ with a probability p_i , the expected value of the block is $[a_1, a_2, a_3, a_4]$ since

$$E[\theta(a_i)] = \frac{a_i}{p_i} \cdot p_i + 0 \cdot (1 - p_i) = a_i \quad (9)$$

for each $i \in \{1, 2, 3, 4\}$

The variance of each element in the pruned block is given as follows:

$$\begin{aligned} \text{Var}[\theta(a_i)] &= E[\theta(a_i)^2] - E[\theta(a_i)]^2 = \\ &= \underbrace{\left(\frac{a_i}{p_i}\right)^2 \cdot p_i + 0^2 \cdot (1 - p_i)}_{E[\theta(a_i)^2]} - a_i^2 = \\ &= \frac{a_i^2}{p_i} - a_i^2 \end{aligned} \quad (10)$$

Therefore, total variance $\text{Var}[\theta] = \text{Var}[\theta(a_1, a_2, a_3, a_4)]$ would be

$$\text{Var}[\theta] = \sum_i \left(\frac{a_i^2}{p_i} - a_i^2 \right) \quad (11)$$

For each $i \in \{1, 2, 3, 4\}$ we have the equality constraint

$$\sum_i p_i - 2 = 0 \quad (12)$$

and inequality constraint:

$$p_i - 1 \leq 0 \quad (13)$$

From KKT conditions:

$$L = \sum_j \left(\frac{a_j^2}{p_j} - a_j^2 \right) + \sum_j \lambda_j (p_j - 1) + \mu \sum_j (p_j - 2) \quad (14)$$

then, taking the derivative with respect to p_i

$$\frac{\partial L}{\partial p_i} = -\frac{a_i^2}{p_i^2} + \lambda_i + \mu = 0 \quad (15)$$

With each i , the constant λ_i could be zero or not. Using Equation 15 for $\lambda_i = 0$ we get that

$$p_i = \frac{a_i}{\sqrt{\mu + \lambda_i}} = \frac{a_i}{\sqrt{\mu}} \quad (16)$$

This coupled with the normalization constraint $\frac{\partial L}{\partial \mu} = 0$ implies that

$$\sum_j p_j = \frac{\sum_j a_j}{\sqrt{\mu}} = 2 \Rightarrow \sqrt{\mu} = \frac{\sum_i a_i}{2} \quad (17)$$

Finally, together with Equation 16 we have that for each $i \in \{1, 2, 3, 4\}$

$$p_i^* = \frac{2a_i}{\sum_i a_i} \quad (18)$$

Turning to the case where $\lambda_i > 0$, we have $p_i - 1 = 0$ (i.e., $p_i^* = 1$) because of the complementary slackness condition. The normalization constraint guarantees that $\sum_{k \neq i} p_k + 1 = 2$ and therefore $\sum_{k \neq i} p_k = 1$ i.e., all other probabilities are in the range $(0, 1)$ and so $\lambda_k = 0$ for every $k, k \neq i$. Therefore, from equation 15 we have that

$$-\frac{a_k^2}{p_k^2} + \mu = 0 \Rightarrow p_k = \frac{a_k}{\sqrt{\mu}} \quad k \neq i \quad (19)$$

Since $\sum_{k \neq i} p_k = 1$ we have that $\sum_{k \neq i} \frac{a_k}{\sqrt{\mu}} = 1$, and therefore $\sqrt{\mu} = \sum_{k \neq i} a_k$. Thus, we can substitute $\sqrt{\mu}$ in Equation 19

$$p_k^* = \frac{a_k}{\sum_{k \neq i} a_k} \quad k \neq i \quad (20)$$

We provide an algorithm in Appendix A.2 for identifying pairs of elements for 2:4 policy that meets the optimization criteria stated in Equations 20 and 18.

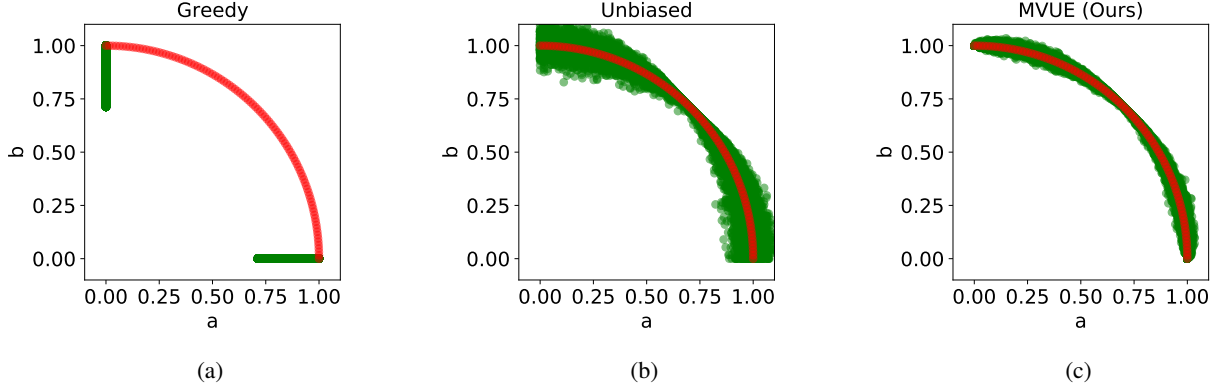


Figure 1. 1:2 Sparsity for blocks located on the first quarter of the unit circle. The blocks $[a,b]$ (represented by red dots) are sampled 100 times each, and then averaged (green dots) using one of three methods: (a) *greedy* is the traditional method that generates the block $[0,b]$ if $a \leq b$, or $[a,0]$ otherwise. In this method, all 100 samples are the same for each block, resulting in a biased average. (b) *unbiased* - each block $[a,b]$ is equally likely to be pruned to $[2a, 0]$ or $[0, 2b]$. Although the average of the 100 samples is unbiased, it does not have minimum variance. (c) Our *unbiased* method with minimum variance (outlined in Equation 35), exhibits a smaller spread here than in (b).

4.3. A comparison of optimal 1:2 and optimal 2:4

Given a block $B = [a_1, a_2, a_3, a_4]$, we can either apply optimal 2:4 method directly on that block $\theta_{2:4}(B)$ or we can break it into two sub-blocks $b_1 = [a_1, a_2]$ and $b_2 = [a_3, a_4]$, and apply optimal 1:2 method twice i.e., $\theta_{1:2}(b_1)$ and $\theta_{1:2}(b_2)$. The following proves that the former alternative is preferable and introduces less variance, i.e.,

$$\text{Var}[\theta_{2:4}(B)] \leq \text{Var}[\theta_{1:2}(b_1)] + \text{Var}[\theta_{1:2}(b_2)] \quad (21)$$

To prove this claim we first find $\text{Var}[\theta_{2:4}(B)]$ by assigning a probability $p_i^* = \frac{a_i}{a_1+a_2+a_3+a_4}$ to each element i in Equation 11:

$$\begin{aligned} \text{var}[\theta^*] &= \frac{a_1}{2} (a_1 + a_2 + a_3 + a_4) - a_1^2 \\ &\quad + \frac{a_2}{2} (a_1 + a_2 + a_3 + a_4) - a_2^2 \\ &\quad + \frac{a_3}{2} (a_1 + a_2 + a_3 + a_4) - a_3^2 \\ &\quad + \frac{a_4}{2} (a_1 + a_2 + a_3 + a_4) - a_4^2 \\ &= a_1 \cdot a_2 + a_1 \cdot a_3 + a_1 \cdot a_4 \\ &\quad + a_2 \cdot a_3 + a_2 \cdot a_4 + a_3 \cdot a_4 \\ &\quad - \frac{a_1^2}{2} - \frac{a_2^2}{2} - \frac{a_3^2}{2} - \frac{a_4^2}{2} \end{aligned} \quad (22)$$

the left hand side of Equation 21 is given by Equation 22 and its right-hand side equals to $2a_1a_2 + 2a_3a_4$. Let D be the difference between the left-handside of Equation 21 and its right hand side. To prove our claim we need to show that

D is negative:

$$\begin{aligned} D &= a_1a_2 + a_1a_3 + a_1a_4 + a_2a_3 + a_2a_4 + a_3a_4 \\ &\quad - \frac{a_1^2}{2} - \frac{a_2^2}{2} - \frac{a_3^2}{2} - \frac{a_4^2}{2} - (2a_1a_2 + 2a_3a_4) \\ &= \underbrace{\left(-\frac{a_1^2}{2} + a_1a_4 - \frac{a_4^2}{2} \right)}_{-0.5(a_1-a_4)^2} + \underbrace{\left(-\frac{a_2^2}{2} + a_2a_3 - \frac{a_3^2}{2} \right)}_{-0.5(a_2-a_3)^2} + \\ &\quad + \underbrace{a_4a_2 + a_1a_3 - a_1a_2 - a_3a_4}_{-(a_1-a_4) \cdot (a_2-a_3)} \end{aligned} \quad (23)$$

Let $A \triangleq (a_1 - a_4)$ and $B \triangleq (a_2 - a_3)$ then we have that

$$D = -\frac{A^2}{2} - A \cdot B - \frac{B^2}{2} = -\frac{1}{2}(A + B)^2 < 0 \quad (24)$$

Our claim is thus proven.

4.4. Approximated optimal 2:4

As shown in Table 6, in terms of time complexity, the optimal method may not be feasible. Using insights gained from the optimal solution, we now present a simple approximation method called approx-MVUE. The idea is simple. We first choose an element a_i with a probability $p_i = \frac{a_i}{a_1+a_2+a_3+a_4}$ and remove a_i from the block. In order to select a second element, we repeat the same procedure for the three remaining elements with probability $p_j = \frac{a_j}{a_1+a_2+a_3+a_4-a_i}$. Thus, each element is chosen with probability:

$$p_i = \frac{|a_i|}{\sum_j |a_j|} + \sum_{k \neq i} \frac{|a_k|}{\sum_j |a_j|} \frac{|a_i|}{\sum_{j \neq k} |a_j|} \quad (25)$$

In order to check the effect of this approximated method to the variance of the estimator, we present in Figure 2 the

ratio of the variance between the two methods: $\frac{\text{Var}(\theta_{2:4}^{\text{approx}})}{\text{Var}(\theta_{2:4}^{\text{opt}})}$, where both variances are calculated analytically using Equation (10)). Without loss of generality for a block $[a_1, a_2, a_3, a_4]$ where $a_1 \leq a_2 \leq a_3 \leq a_4$, we set $a_4 = 1$ and scan with small steps all combinations of a_1, a_2, a_3 . The scan suggests the variance ratio is bounded below two¹, and therefore the approximate method is a 2-approximation of the old method. As can be seen in Table 6 the approximated method reduces the complexity time of MVUE 2:4 by $\sim 70\%$, in our non-optimized implementation.

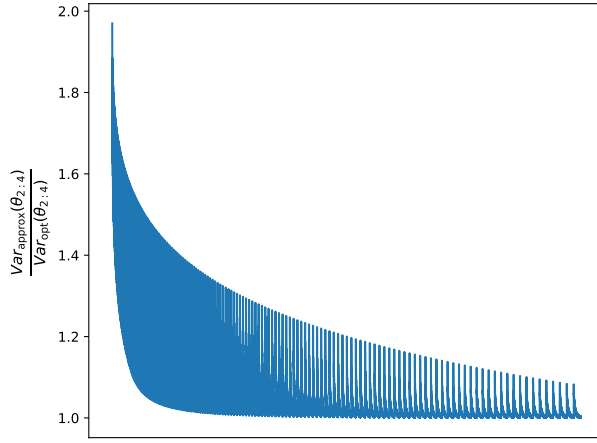


Figure 2. Ratio between the variance (Equation (10)) of the approx-MVUE 2:4 and MVUE 2:4 in a scan of all possible values of the block $[a_1, a_2, a_3, 1]$, where $0 \leq a_1, a_2, a_3 \leq 1$ with a step size 0.005. Notice that ratio is bounded below 2. The maximum is achieved near the left edge, when $a_4 \ll \max(a_1, a_2, a_3)$.

5. Hardware Constraints

So far fine-grained sparsity papers focused on pruning only the weights matrix (Nvidia, 2020; Zhou et al., 2021; Hubara et al., 2021). Here we investigate pruning gradients and activations as well. Therefore, we need to understand how much acceleration can we expect, when both matrices involve in the matrix multiplication are fine-grained pruned. Assuming we have two N:M fine-grained blocks b_W b_x with masks M_{b_W} and M_{b_x} , the number of Multiply and Accumulate operations (MACs) required for multiplying and accumulating the blocks may vary from zero to N. For example for 2:4 fine-grained sparsity, there are $\binom{4}{2} = 6$ possible mask configuration. Thus, the expected number of MACs in a block, assuming uniform distribution on the non-zeros in

¹The largest values are near the left edge of the scan, which represents the limit where $a_4 \gg a_1, a_2, a_3$. Near this edge, we additionally checked with very small (logarithmically spaced) step sizes that the variance ratio is bounded below two.

the blocks, would be:

$$\begin{aligned} \mathbb{E}[\#\text{MACs}(b_x, b_W)] &= \mathbb{E}[\mathbb{E}[\#\text{MACs}(b_x, b_W) | M_{b_x}]] \\ &= \frac{1}{6} \cdot 0 + \frac{1}{6} \cdot 2 + \frac{4}{6} \cdot 1 = 1 \end{aligned} \quad (26)$$

Thus on average, each block contains $N/2$ MACs. While some architectures (such as CPU) can avoid all unnecessary multiplication, architectures with a systolic array at the core of their matrix multiplication engine must always assume the worst case. Therefore, for these types of architectures, we cannot achieve an additional compute reduction by pruning both matrices involved in the matrix multiplication. Yet, the bandwidth reduction for both matrices is the same. This property helps support sparse and dense matrix multiplication without creating dedicated hardware which has twice the bandwidth to one of the matrices. It is specifically important when targeting higher sparsity. For instance, if only the weights obey 1:4 fine-grained structure then the activations bandwidth is 4x higher than the weights bandwidth as for every single block we bring one weight and four activations to the engine.

Additionally, we noticed that doing N:M fine-grained sparsity on the activations is not useful for accelerating the update phase, since: (1) we must sparsify the activations for each sample separately (for inference), and (2) our experiments indicated that structured sparsity on the spatial dimension does not work well. In contrast, neural gradients can be sparsified in the batch dimension, and so can accelerate the update phase.

6. Experiments

In this section, we demonstrate the effectiveness of our proposed methods over several vision models. First we show the effect of the proposed method for the fine-grained N:M structured sparsity on the neural gradients and demonstrate results when combined with the fine-grained N:M transposable weight (Hubara et al., 2021) allowing for the first time the acceleration with N:M structured sparsity in all training GEMM. Then we show the results of applying greedy fine-grained N:M structured sparsity on the activations and finally combined the greedy fine-grained N:M structured sparsity on the weights and activations to achieve near state-of-the-art results in the deployment of a model that is similar to 2-bit quantization in terms of bit-operations(BOPS) (Wang et al., 2020).

6.1. N:M structured sparsity on the neural gradients

In Figures 3 and 4 we showed the results of applying the suggested N:M structured sparsity for ResNet18 and ResNet50 ImageNet dataset respectively. The 1:2 results refer to the MVUE method (Section 4.1) while the 2:4 results refer to

the approximate method (Section 4.4). In Figure 3 we compare the proposed method also with the traditional greedy method of keeping the largest elements in each block. While the greedy method had a very significant degradation, the proposed method achieved baseline accuracy with the simple MVUE 1:2. Additional experiments appear in the Appendix A.3.

We used the standard pre-processing of ImageNet ILSVRC2012 dataset. We train for 90 epochs, use an initial learning rate of 0.1 with a $\frac{1}{10}$ decay at epochs 30,60,80. We use standard SGD with momentum of 0.9 and weight decay of 1e-4. The batch size used is 256. Following the DNNs quantization conventions (Banner et al., 2018; Nahshan et al., 2019; Choi et al., 2018b) we kept the first and last layer (FC) at higher precision.

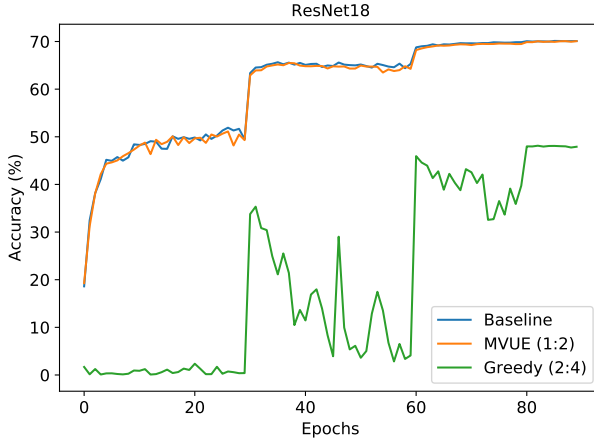


Figure 3. Top-1 validation accuracy in ResNet18 ImageNet dataset with the suggested fine-grained structured sparsity MVUE 1:2. We compare it with the traditional greedy 2:4 method of keeping the two larger elements in each block of size four. While the MVUE 1:2 has no degradation, the greedy 2:4 get a big degradation.

6.2. Accelerating all training phases

In Table 3 we showed the results of the combination between the proposed N:M MVUE for the neural gradients and the N:M transposable weights presented in (Hubara et al., 2021). The combination between both methods allowed for the first time to accelerate with N:M structured sparsity for all training GEMM operations. This demonstrates that one can achieve 2x acceleration in all training with minimal or no accuracy degradation. In these experiments, we used the exact same experiment setting as Hubara et al. (2021).

6.3. N:M structured sparsity on the activations

We experimented with greedy N:M fine-grained sparse activations on ResNet18 and ResNet50 over ImageNet, wherein

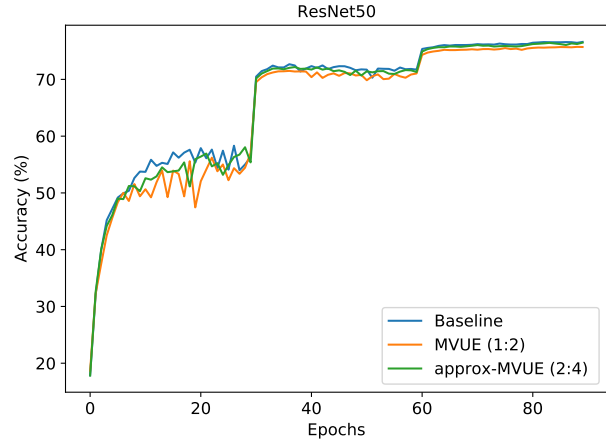


Figure 4. Top-1 validation accuracy of ResNet50 trained over ImageNet dataset with the suggested fine-grained structured sparsity using MVUE 1:2 and approx-MVUE 2:4 criteria for the neural gradients. The MVUE 1:2 gets degradation of 0.8% while the approx-MVUE 2:4 achieved baseline accuracy.

Table 3. Top-1 validation accuracy on ImageNet dataset of the combination of the suggested MVUE 1:2 and approx-MVUE 2:4 with the transposable weights of Hubara et al. (2021). While the transposable weights enable accelerating the forward and backward phases, the suggested methods are able to accelerate the update phase. With this combination, we are able to accelerate for the first time all training phases with N:M fine-grained structured sparsity.

Model	G	W^T	Acc (%)
ResNet18	FP32	FP32	70.6
	FP32	2:4	70.5
	1:2	2:4	70.4
	2:4	2:4	70.6
ResNet50	FP32	FP32	77.2
	FP32	2:4	77.1
	1:2	2:4	75.6

for each block of size M we keep the M-N bigger elements. Note that in CNNs the activations memory footprint is much larger than the weights footprint (especially for the first set of layers). Throughout our experiments, we did not change the training regime and applied the sparsity from scratch. Since the training regimes and model initialization are tailored to the ReLU function our pruning criterion was the activation value and not its absolute value (i.e., magnitude). As can be seen in Figure 5 applying only fine-grained sparsity results in notable accuracy degradation for both training and validation. However, a simple fix that requires only to apply ReLU before the fine-grained sparsity results in on par accuracy over ResNet18 and ResNet50 (Table 4).

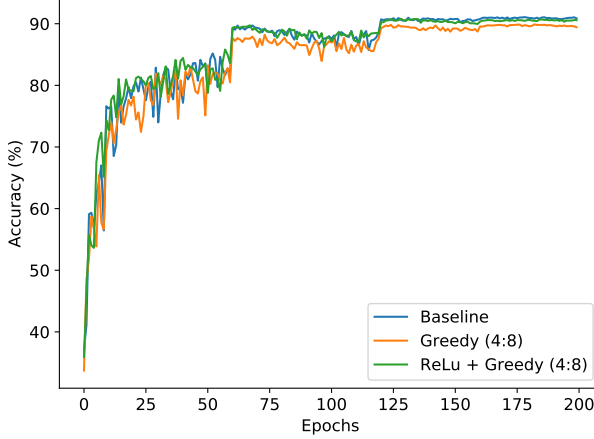


Figure 5. Top-1 accuracy on ResNet18 Cifar10 dataset with 4:8 fine-grained sparsity. ReLU + greedy refers to applying ReLU and then the structured sparsity, while greedy does not include the ReLU function. As can be seen, applying only N:M structured sparsity as the activation function leads to accuracy degradation.

Table 4. ResNet18 (R18) and ResNet50 (R50) top-1 accuracy on ImageNet dataset with greedy N:M fine-grained sparsity on the activations

Method	R18 top-1 (%)	R50 top-1 (%)
Baseline	70.6	76.6
4:8 activations	70.6	76.45

6.4. Accelerating inference

Accelerating inference requires compressing only the weights and activations. Thus, we experimented in Table 5 with greedy N:M fine-grained sparsity of weight and activations. To compete with the latest inference acceleration results based on quantization-aware techniques, we further quantize the weights and activation to 4-bit using the SAWB method (Choi et al., 2018a). Since on average we have $N/2$ MAC operations for each block, the BOPS (Wang et al., 2020) reduction is equivalent to 2-bit quantization. We experimented with N:M fine-grained sparse activations and weights using ResNet18 over ImageNet using two training schemes:

- **Scheme A** is similar to Zhou et al. (2021) regime in which sparse weights are used from scratch only here we additionally applied 4-bit asymmetric quantization for both weights and activations.
- **Scheme B** is similar to Nvidia (2020) regime and has three phases: (a) train a sparse activation full precision model; (b) set a mask for the weights; and (c) train a sparse weights and activation model while using 4bit

quantization-aware training.

In all our experiments we kept last fully connected layer dense and in full precision. We used 2:4 structure for the weights and 4:8 structure for the activations.

Table 5. Inference acceleration of ResNet18 on ImageNet dataset. We quantize the weights and activations to 4-bit and apply in both greedy N:M fine-grained sparsity getting an equivalent of 2-bit inference. We compare our results with different 2-bit quantization-aware training methods.

Method	Accuracy (%)
Baseline	70.6
4:8 activations	70.6
Scheme A (ours)	66.5
Scheme B (ours)	67.33
PACT 2-bit (Choi et al., 2018b)	64.4
QIL 2-bit (Jung et al., 2019)	65.7
LSQ 2-bit (Esser et al., 2019)	66.9

7. Discussion

In this work, we studied the effect of N:M structured sparsity on the neural gradients and activations:

Sparse Gradients Basing on a previous work (Chmiel et al., 2021b) which show the importance of unbiasedness of the neural gradients, we suggest an unbiased minimum variance method to prune the neural gradient with 1:2 and 2:4 structured sparsity. Moreover, since the optimal 2:4 method may not be feasible in term of complexity, we suggest an approximate method which increases the variance only by a factor of 2 (making it a 2-approximation). We showed that our method achieved small or no degradation while the traditional greedy method completely failed. Moreover, we combine our method with a previous method for transposable weights (Hubara et al., 2021). This enabled N:M fine grained sparsity, for the first time, to accelerate by 2x with all training process.

Sparse Activations. ReLU is a very common activation function that usually combined with some normalization function (e.g., batch norm). Thus commonly applying ReLU result in 50% sparse output. Here for the first time we investigate fine-grained N:M sparsity for the activations. While simply applying N:M sparsity on the pre-ReLU outputs results in severe degradation, using ReLU and then enforcing the structure result in an on-par accuracy. Notably, N:M structured sparsity in the activations can lead to acceleration of the proceeding layer’s backward phase (in our case batch-norm) as the gradient’s share the same mask. We

experimented with different training regimes and initialization schemes for fine-grained sparse activation but did not observe accuracy boost. Finally, we suggested for inference to use weights and activation that are fine-grained sparse and quantized.

References

Aamir Raihan, M. and Aamodt, T. M. Sparse weight activation training. *arXiv preprint arXiv:2001.01969*, 2020. URL <http://arxiv.org/abs/2001.01969>.

Banner, R., Hubara, I., Hoffer, E., and Soudry, D. Scalable methods for 8-bit training of neural networks. In *NeurIPS*, 2018.

Chmiel, B., Banner, R., Hoffer, E., Yaacov, H. B., and Soudry, D. Logarithmic unbiased quantization: Practical 4-bit training in deep learning. *ArXiv*, abs/2112.10769, 2021a.

Chmiel, B., Ben-Uri, L., Shkolnik, M., Hoffer, E., Banner, R., and Soudry, D. Neural gradients are lognormally distributed: understanding sparse and quantized training. In *ICLR*, 2021b.

Choi, J., Chuang, P., Wang, Z., Venkataramani, S., Srinivasan, V., and Gopalakrishnan, K. Bridging the accuracy gap for 2-bit quantized neural networks (qnn). *ArXiv*, abs/1807.06964, 2018a.

Choi, J., Wang, Z., Venkataramani, S., Chuang, P., Srinivasan, V., and Gopalakrishnan, K. Pact: Parameterized clipping activation for quantized neural networks. *ArXiv*, abs/1805.06085, 2018b.

Esser, S. K., McKinstry, J. L., Bablani, D., Appuswamy, R., and Modha, D. S. Learned step size quantization. *arXiv preprint arXiv:1902.08153*, 2019.

Evci, U., Gale, T., Menick, J., Castro, P. S., and Elsen, E. Rigging the lottery: Making all tickets winners. In *International Conference on Machine Learning*, pp. 2943–2952. PMLR, 2020.

Frankle, J. and Carbin, M. The lottery ticket hypothesis: Finding sparse, trainable neural networks. In *ICLR*, 2018.

Holmes, C., Zhang, M., He, Y., and Wu, B. Nxmtransformer: Semi-structured sparsification for natural language understanding via admm. *ArXiv*, abs/2110.15766, 2021.

Hubara, I., Chmiel, B., Island, M., Banner, R., Naor, S., and Soudry, D. Accelerated sparse neural training: A provable and efficient method to find n: M transposable masks. In *NeurIPS*, 2021.

Janowsky, S. A. Pruning versus clipping in neural networks. *Physical Review A*, 39(12):6600–6603, 1989. URL <https://link.aps.org/doi/10.1103/PhysRevA.39.6600>.

Jaszczerzak, S., Chowdhery, A., Mohiuddin, A., Kaiser, L., Gajewski, W., Michalewski, H., and Kanerva, J. Sparse is enough in scaling transformers. 2021.

Jung, S., Son, C., Lee, S., Son, J., Han, J.-J., Kwak, Y., Hwang, S. J., and Choi, C. Learning to quantize deep networks by optimizing quantization intervals with task loss. In *Proceedings of the IEEE/CVF Conference on Computer Vision and Pattern Recognition*, pp. 4350–4359, 2019.

Kurtz, M., Kopinsky, J., Gelashvili, R., Matveev, A., Carr, J., Goin, M., Leiserson, W., Moore, S., Shavit, N., and Alistarh, D. Inducing and exploiting activation sparsity for fast inference on deep neural networks. In III, H. D. and Singh, A. (eds.), *Proceedings of the 37th International Conference on Machine Learning*, volume 119 of *Proceedings of Machine Learning Research*, pp. 5533–5543. PMLR, 13–18 Jul 2020. URL <https://proceedings.mlr.press/v119/kurtz20a.html>.

Leclerc, G., Ilyas, A., Engstrom, L., Park, S. M., Salman, H., and Madry, A. ffcv. <https://github.com/libffcv/ffcv/>, 2022. commit xxxxxxxx.

Li, H., Kadav, A., Durdanovic, I., Samet, H., and Graf, H. P. Pruning filters for efficient convnets. In *ICLR*, 2017.

Liu, Z., Sun, M., Zhou, T., Huang, G., and Darrell, T. Rethinking the value of network pruning. *arXiv preprint arXiv:1810.05270*, 2018.

Luo, J.-H., Wu, J., and Lin, W. Thinet: A filter level pruning method for deep neural network compression. *2017 IEEE International Conference on Computer Vision (ICCV)*, pp. 5068–5076, 2017.

McDanel, B., Dinh, H., and Magallanes, J. R. Accelerating dnn training with structured data gradient pruning. *ArXiv*, abs/2202.00774, 2022.

Mishra, A. K., Latorre, J. A., Pool, J., Stosic, D., Stosic, D., Venkatesh, G., Yu, C., and Micikevicius, P. Accelerating sparse deep neural networks. *ArXiv*, abs/2104.08378, 2021.

Nahshan, Y., Chmiel, B., Baskin, C., Zheltonozhskii, E., Banner, R., Bronstein, A. M., and Mendelson, A. Loss aware post-training quantization. *arXiv preprint arXiv:1911.07190*, 2019. URL <http://arxiv.org/abs/1911.07190>.

Nvidia. a100 tensor core gpu architecture. 2020. URL <http://https://www.nvidia.com/content/dam/en-za/Solutions/Data-Center/nvidia-ampere-architecture-whitepaper.pdf>.

Pool, J. and Yu, C. Channel permutations for n:m sparsity. In *NeurIPS*, 2021.

Renda, A., Frankle, J., and Carbin, M. Comparing rewinding and fine-tuning in neural network pruning. *ArXiv*, abs/2003.02389, 2020.

Stosic, D. and Stosic, D. Search spaces for neural model training. *ArXiv*, abs/2105.12920, 2021.

Sun, W., Zhou, A., Stuijk, S., Wijnhoven, R. G. J., Nelson, A., Li, H., and Corporaal, H. Dominosearch: Find layer-wise fine-grained n:m sparse schemes from dense neural networks. In *NeurIPS*, 2021. URL https://openreview.net/forum?id=IGrC6koW_g.

Sun, X., Ren, X., Ma, S., and Wang, H. meprop: Sparsified back propagation for accelerated deep learning with reduced overfitting. In *ICML*, 2017.

Wang, Y., Lu, Y., and Blankevoort, T. Differentiable joint pruning and quantization for hardware efficiency. In *European Conference on Computer Vision*, pp. 259–277. Springer, 2020.

Wen, W., Wu, C., Wang, Y., Chen, Y., and Li, H. Learning structured sparsity in deep neural networks. In *In Advances in neural information processing systems*, pp. 2074–2082, 2016.

Ye, X., Dai, P., Luo, J., Guo, X., Qi, Y., Yang, J., and Chen, Y. Accelerating cnn training by pruning activation gradients. *arXiv preprint arXiv:1908.00173*, 2019. URL <http://arxiv.org/abs/1908.00173>.

Zhou, A., Ma, Y., Zhu, J., Liu, J., Zhang, Z., Yuan, K., Sun, W., and Li, H. Learning n:m fine-grained structures sparse neural networks from scratch. In *ICLR*, 2021.

A. Appendix

A.1. 1:2 minimum variance unbiased estimator- Full

For a block $[a, b]$, one entry needs to be pruned:

$$\theta([a, b]) = \begin{cases} [v_1, 0] & , \text{w.p. } p \\ [0, v_2] & , \text{w.p. } 1 - p \end{cases} \quad (27)$$

We wish to design an unbiased estimator for this pruning method where $E[\theta([a, b])] = [a, b]$:

$$E[\theta([a, b])] = p \cdot [v_1, 0] + (1 - p) \cdot [0, v_2] = [a, b] \quad (28)$$

Therefore, the following constraints apply:

$$\begin{aligned} p \cdot v_1 &= a & \Rightarrow p &= \frac{a}{v_1} \\ (1 - p) \cdot v_2 &= b & \Rightarrow v_2 &= \frac{b}{1 - \frac{a}{v_1}} \end{aligned} \quad (29)$$

To find an unbiased estimator which minimizes the total block variance, we first calculate the variance for each element in the block $\theta([a, b]) = [x, y]$ as follows:

$$\begin{aligned} \text{Var}[x] &= E[x^2] - E^2(x) = v_1^2 \cdot p - a^2 \\ \text{Var}[y] &= E[y^2] - E^2[y] = v_2^2 \cdot (1 - p) - b^2 \end{aligned} \quad (30)$$

Then, the total variance of a block is the sum of its element variances:

$$\text{Var}_B[\theta] = \text{Var}[x] + \text{Var}[y] = v_1^2 p - a^2 + v_2^2 (1 - p) - b^2 \quad (31)$$

Putting equation 29 into equation 31 yields the following expression for the total variance in the block that depends on v_1

$$\begin{aligned} \text{Var}_B[\theta] &= v_1^2 \cdot \frac{a}{v_1} - a^2 + \frac{b^2}{\left(1 - \frac{a}{v_1}\right)^2} \cdot \left(1 - \frac{a}{v_1}\right) - b^2 \\ &= v_1 \cdot a - a^2 + \frac{b^2}{1 - \frac{a}{v_1}} - b^2 \\ &= v_1 \cdot a - a^2 + \frac{b^2 \cdot v_1}{v_1 - a} - b^2 \end{aligned} \quad (32)$$

By finding the derivative of equation 32 with respect to v_1 and setting it to zero we get the following equation:

$$\frac{\partial \text{Var}_B[\theta]}{\partial v_1} = \frac{b^2}{v_1 - a} - \frac{b^2 v_1}{(v_1 - a)^2} + a = 0 \quad (33)$$

The solution to equation 33 gives two possible solutions for v_1 , but only one is feasible (the first):

$$\begin{aligned} v_1^* &= a + b \\ v_1^* &= a - b \end{aligned} \quad (34)$$

Therefore, the following unbiased estimator has the lowest variance of all unbiased estimators

$$\theta([a, b]) = \begin{cases} [\text{sign}(a) \cdot (|a| + |b|), 0] & , \text{w.p. } \frac{|a|}{|a| + |b|} \\ [0, \text{sign}(b) \cdot (|a| + |b|)] & , \text{w.p. } \frac{|b|}{|a| + |b|} \end{cases} \quad (35)$$

Substituting into Equation 32 the optimal solution $v_1^* = a + b$, the optimal method outlined in 35 has a variance of $2ab$. Therefore, since the method is unbiased it results with a mean-square-error of

$$MSE = \text{Bias}^2 + \text{Var} = 0 + 2ab = 2ab \quad (36)$$

In Table 2 we compare different 1:2 structured sparsity on the neural gradients on ResNet18 Cifar10 dataset. We show that although the proposed MVUE method doesn't minimize the MSE, it gets the best results.

A.2. minimum-variance unbiased algorithm for 2:4

Given a block $[a_1, a_2, a_3, a_4]$, assume without loss of generality that $a_4 > a_3 > a_2 > a_1$. We need to choose two elements a_i, a_j from the block with a probability $p_{i,j}$. We have three cases:

A.2.1. CASE 1: $a_4 \leq 2a_1 + a_3$:

$$\begin{aligned} p_{12} &= 0 \\ p_{13} &= \frac{2a_1 + a_3 - a_4}{2(a_1 + a_2 + a_3 + a_4)} \\ p_{14} &= \frac{2a_1 - a_3 + a_4}{2(a_1 + a_2 + a_3 + a_4)} \\ p_{23} &= \frac{2a_2 + a_3 - a_4}{2(a_1 + a_2 + a_3 + a_4)} \\ p_{24} &= \frac{2a_2 - a_3 + a_4}{2(a_1 + a_2 + a_3 + a_4)} \\ p_{34} &= \frac{-a_1 - a_2 + a_3 + a_4}{a_1 + a_2 + a_3 + a_4} \end{aligned} \tag{37}$$

Using the above solution, one can verify that all probabilities are between 0 and 1, normalized, and adhere to the optimality conditions outlined in Equation (18). Here is an example for p_1 and p_2 :

$$\frac{p_1}{p_2} = \frac{p_{12} + p_{13} + p_{14}}{p_{12} + p_{23} + p_{24}} = \frac{a_1}{a_2} \tag{38}$$

A.2.2. CASE 2: $2a_1 + a_3 \leq a_4 \leq a_1 + a_2 + a_3$:

$$\begin{aligned} p_{12} &= 0 \\ p_{13} &= 0 \\ p_{14} &= \frac{2a_1}{a_1 + a_2 + a_3 + a_4} \\ p_{23} &= \frac{a_1 + a_2 + a_3 - a_4}{a_1 + a_2 + a_3 + a_4} \\ p_{24} &= \frac{-a_1 + a_2 - a_3 + a_4}{a_1 + a_2 + a_3 + a_4} \\ p_{34} &= \frac{-a_1 - a_2 + a_3 + a_4}{a_1 + a_2 + a_3 + a_4} \end{aligned} \tag{39}$$

A.2.3. CASE 3: $a_4 \geq a_1 + a_2 + a_3$:

Choose a_4 with probability 1, and also choose one a_i from $\{a_1, a_2, a_3\}$ with probability

$$\tilde{p}_i = \frac{a_i}{a_1 + a_2 + a_3} \tag{40}$$

A.3. Additional experiments

In Figure 6 we show the top-1 accuracy of ResNext50 with the proposed MVUE(1:2) method, achieving a small degradation (1%).

A.4. Comparison with SDGP (McDaniel et al., 2022)

In parallel to our work, (McDaniel et al., 2022), proposed to prune the neural gradients to accelerate only the backward phase, while the update and forward phase are not pruned. Their method is based on the traditional greedy method, followed

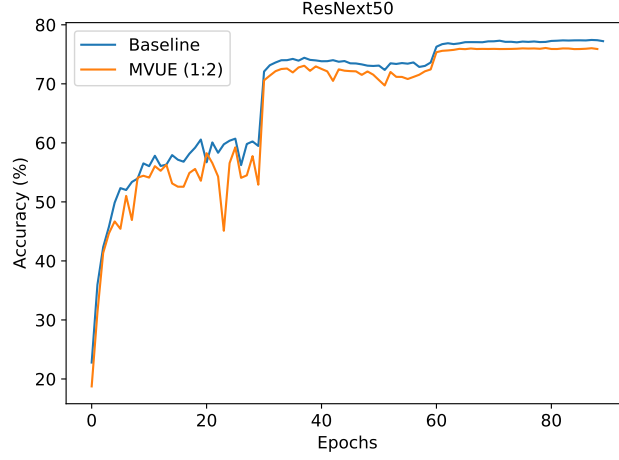


Figure 6. Top-1 validation accuracy in ResNext50 ImageNet dataset with the suggested fine-grained structured sparsity MVUE 1:2.

Table 6. Overhead of different algorithms for finding the required masks: ratio of their running time over regular training (ResNet50). Notice the overhead reduction in the Approx-MVUE 2:4 in comparison to MVUE 2:4. All experiments were run without sparse-tensor cores and in a non optimized implementation.

Method	Overhead (%)
MVUE 1:2	15 %
MVUE 2:4	95 %
Approx-MVUE 2:4	27 %

by a rescaling of the remaining elements to keep the l_1 norm. In order to check the effect of their method we show in Table 7 the results of applying SDGP also in the update phase. As can be seen, while their method works well in the backward phase, their biased method creates a high degradation in the update phase. Notice that in all their experiments they use FFCV (Leclerc et al., 2022) training regime, which achieves a higher baseline.

Table 7. ResNet18 top-1 validation accuracy in ImageNet dataset while applying SDGP (McDanel et al., 2022) in the backward and update phases.

Method	Accuracy (%)
Baseline	71.4 %
SDGP backward	71.2 %
SDGP update	64.2 %